

Problem Space Transformations for Out-of-Distribution Generalisation in Behavioural Cloning

Kiran Doshi¹, Marco Bagatella¹ and Stelian Coros¹

Abstract—The combination of behavioural cloning and neural networks has driven significant progress in robotic manipulation. As these algorithms may require a large number of demonstrations for each task of interest, they remain fundamentally inefficient in complex scenarios, in which finite datasets can hardly cover the state space. One of the remaining challenges is thus out-of-distribution (OOD) generalisation, i.e. the ability to predict correct actions for states with a low likelihood with respect to the state occupancy induced by the dataset. This issue is aggravated when the system to control is treated as a black-box, ignoring its physical properties. This work highlights widespread properties of robotic manipulation, specifically pose equivariance and locality. We investigate the effect of the choice of problem space on OOD performance of BC policies and how transformations arising from characteristic properties of manipulation can be employed for its improvement. Through controlled, simulated and real-world experiments, we empirically demonstrate that these transformations allow behaviour cloning policies, using either standard MLP-based one-step action prediction or diffusion-based action-sequence prediction, to generalise better to certain OOD problem instances. Code is available at https://github.com/kirandoshi/pst_ood_gen.

I. INTRODUCTION

The behavioural cloning (BC) paradigm [1], [2] has been the foundation of recent advances in robotic manipulation [3], [4], [5]. BC is particularly promising for robot manipulation, as humans are very proficient in general manipulation, and can quickly learn to collect demonstrations when given a well-designed interface [6]. An important benefit of using this data to train a robot policy is that it can be collected on the real system, thus avoiding the sim-to-real gap. However, as a supervised learning method, BC requires the collected data to cover the workspace with relatively high density [7], [8], [9]. Neural networks trained with BC, and more generally functions estimated through supervised learning, hardly generalise outside the support of the training data, i.e. "out-of-distribution" (OOD) [10], [11]. Avoiding OOD states by providing sufficient data coverage can quickly become infeasible. This is particularly aggravating for robotic manipulation, as collection of human demonstrations remains time intensive and thus expensive [4].

The aim of this work is to investigate the effect of the choice of the problem space on the ability of a BC policy to generalize OOD. The focus is on robotic manipulation tasks with rigid bodies and low-dimensional state information. Therefore, practical assumptions on object-centric manipulation tasks are highlighted and leveraged to explore a family

of associated problem space transformations. We observe that these transformations are a crucial design component for learning-based control of manipulators, and enable policies learned through BC to perform well on OOD states. Our focus is not that of solving OOD generalisation as a whole, but rather to carefully evaluate how careful transformation of the problem space in a common setup impacts generalization.

We thus present three main contributions:

- we formalise the OOD problem in the context of manipulation;
- we describe several transformations of the problem space that embed these properties;
- we provide experimental results demonstrating that the choice of problem space transformation significantly impacts the ability of OOD generalisation for three simulated robotic manipulation tasks and a real-world pushing task.

After introducing related works and preliminaries in Sections II and III respectively, we present our main contributions in Section IV and validate it empirically in Section V. An overview of the proposed problem space transformations can be seen in Figure 1.

II. RELATED WORK

a) Imitation Learning and Behavioural Cloning: The core idea of imitation learning is that of extracting a control policy from high-quality data [12], [13]. Imitating expert trajectories can be framed in various formulations, encompassing both offline [2], [14] and online [15], [16] methods. A core technique that has recently risen to prominence is that of behavioural cloning (BC) [1], [2], which casts the problem as supervised learning, and optimizes a policy by minimizing the distance of its output to expert actions. Due to its offline nature, BC notoriously suffers from accumulating errors [2]. However, BC has been instrumental to multiple recent advances in robotic manipulation [6], [4], in which good demonstrations can be easily collected [17]. In this context, diffusion-based parametrizations [3] have arisen as an expressive policy class, capable of modelling multi-modal behaviours. Finally, formal understanding of BC has also gradually advanced [18], [19], and performance guarantees have become more practical [20], [21].

b) Using Robotic Manipulation Properties in Policy Learning: Past work has explored exploiting different invariances and equivariances in robot manipulation learning. In [22], learnt SE(3)-equivariant object representations, which have an object point cloud as input, are deployed to enable

¹All authors are part of the Department of Computer Science at ETH Zürich, Zürich, Switzerland. All correspondence to doshik@ethz.ch.

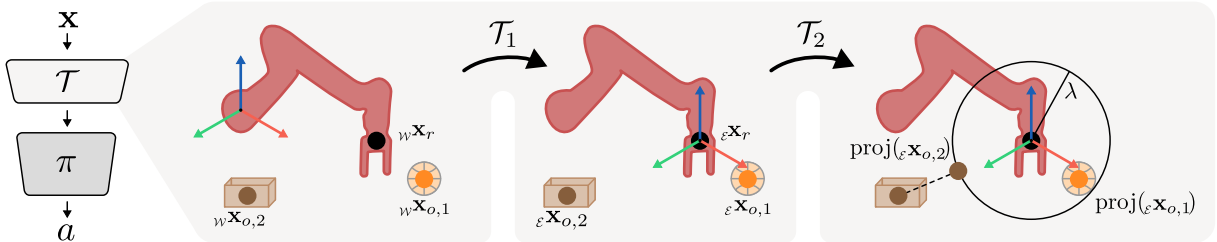


Fig. 1. Overview of the proposed transformations of the behaviour cloning problem space. The base problem space is with a (arbitrary, e.g. at the base of the robot) fixed Cartesian coordinate system \mathcal{W} in which the pose of the end-effector as well as the objects are measured. \mathcal{T}_1 transforms the problem space such that all poses are measured with respect to the moving Cartesian frame of the end-effector \mathcal{E} . \mathcal{T}_2 projects all values to a λ -ball centred at the origin of \mathcal{E} .

a pick and place system that requires only a few demonstrations. In [23], SIM(3) equivariance (which additionally to SE(3) includes scale equivariance) is embedded in the object representation learning module (again from point clouds) as well as in the BC policy network module. The work in [24] takes a similar approach, though adding a SIM(3)-equivariant Diffusion Policy as the BC policy module. Recent work additionally explores the usefulness of the *locality* of manipulation problems to increase sample efficiency by predicting actions as displacements to points in the scene point cloud [25] (thus assuming 3D sensing) or by leveraging gaze data [26]. Some past work also looks at the benefits of introducing SO(2)-equivariance to online [27] and offline RL [28] where the scene entity poses are assumed to be available.

c) Out-of-Distribution Generalisation: A large interest was taken in the problem of OOD generalisation (sometimes also called domain generalisation) in the area of image classification, where pure empirical risk minimisation (ERM) would, for instance, produce classifiers relying on the background instead of the subject of an image [29]. A prominent paradigm is to view the problem as a minimization of the worst-case error over a set of possible environments, with the aim to perform well across all of them [30]. This approach, called Invariant Risk Minimization (IRM), aims to find a predictor which balances prediction accuracy with invariance across different environments. Further work such as [31] and [32] have built upon IRM. An alternative line of work views the data as a composition of semantic and non-semantic components [33], [34]. In this case, the learned predictors should perform well when there is a covariate shift in the non-semantic distribution. For this purpose, [33] assume the existence of minority and majority groups in the data, and introduce a loss term encouraging similar predictive distributions over both groups. A related work in the context of sequential decision making [34] disentangles semantic components in images by assuming access to a reward function that is informative of the nature of the task. These works assume that the dataset includes additional structure which provides implicit direction for a method to determine robust features. Our work aims to solve a related, but different problem: the objective is known (i.e., extending the range of robotic tasks), but no additional information is available except for state-action trajectories (see IV). We thus propose to leverage general inductive biases specific to physical systems, rather than instance-specific information which is, in our case, not available.

III. PRELIMINARIES

A. Behavioural Cloning

We assume that the data is collected in a finite-horizon Markov Decision Process (MDP) modelled as tuple $\mathcal{M} = (\mathcal{X}, \mathcal{A}, P, \mathcal{R}, \mu_0, H)$, where \mathcal{X} is the state space, \mathcal{A} is the action space, $\mathcal{R} : \mathcal{X} \times \mathcal{A} \rightarrow \mathbb{R}$ is the reward function, $P : \mathcal{X} \times \mathcal{A} \rightarrow \Delta(\mathcal{X})$ is the dynamics transition probability function, $\mu_0 \in \Delta(\mathcal{X})$ is the initial state distribution and H is the horizon. BC learns a stationary parameterised policy $\pi_\theta : \mathcal{X}^{T_X} \rightarrow \mathcal{A}^{T_A}$ from a dataset of K task rollouts $\mathcal{D} = \{\tau_1, \dots, \tau_K\}$ with $\tau_k = \{(x_0, a_0), \dots, (x_H, a_H)\}$, $x_0 \sim \mu_0$, $x_{t+1} \sim P(x_t, a_t)$ and $a_t \sim \pi_d(s_t)$. In this case π_d represents the demonstrator's policy. In the general case, the policy predicts a sequence of actions with T_A steps based on an state sequence with T_X steps. We utilise two different methods to train BC policies in this work. (i) The first assumes that $T_X = T_A = 1$. In that case, the policy π_θ is a deterministic multi-layer perceptron (MLP) and is trained by regressing actions with a loss function $\mathcal{L} = \sum_{(x,a) \in \mathcal{D}} D(a, \pi_\theta(x))$, where D is an appropriate distance metric. (ii) In the second case we allow both to be larger than 1, i.e. $T_X > 1$, $T_A > 1$. In this case the policy is trained as a Denoising Diffusion Probabilistic Model, which is known as a *Diffusion Policy* [3]. In both cases the loss constitutes a *proxy* objective, as the actual goal is to maximise the policy's returns: $\mathbb{E}_{\mu_0, \pi_\theta, P} \sum_{t=0}^{H-1} R(x_t, a_t)$.

B. Robotic Manipulation and Problem Space

In this work, we consider robotic manipulation tasks. We define the space of state-action tuples as the problem space $\mathcal{P} = \mathcal{X} \times \mathcal{A}$. As multiple MDPs can model the same environment, the problem space is generally chosen by the designer of the system. A common choice of state and action space by practitioners is as follows [35]. The state space will include proprioceptive information \mathbf{x}_r , e.g. in the form of joint positions or the end-effector (EE) pose. Furthermore, the poses of the entities in the scene would be included, resulting in $\mathbf{x} = [\mathbf{x}_r, (\mathbf{x}_{o,i})_1^{N_O}]$, where N_O is the number of entities. The action space is usually a set point for the low level robot control, either at joint or at EE level $\mathbf{a} = [\mathbf{a}_r]$. As forward and inverse kinematics (calculation of EE pose from joint position values and its inverse) are usually accessible, we assume that both action and proprioception are expressed as EE poses without loss of generality. We also assume that the action is given as an offset to the current EE position, though it is also common to include it as the next EE position or as a velocity. We leave out the state and change of the



Fig. 2. Visualisation of the effect of the proposed transformation on the in-distribution manifold $\hat{\mathcal{X}}$ and on the desired manifold \mathcal{X}^* . The aim is that in the transformed space both manifolds are aligned such that OOD states in \mathcal{P} receive supervision signal in \mathcal{Q} .

gripper in state and action space respectively for the sake of brevity. While we focus on this specific setting due to its prominence in learning-based robotics, we remark that several other problem spaces are common, each of which would induce different properties and transformations.

C. Out of Distribution Generalisation and BC

Out-of-distribution (OOD) generalisation is the desirable capability of a model to return reasonable predictions for unseen data points. We provide a practical, more specific definition in the context of this work. As the learned model π_θ operates over states, we introduce a state occupancy $\Omega \in \Delta(\mathcal{S})$ such that samples in the dataset \mathcal{D} can be considered to be drawn independently and identically distributed (iid) from it. For a given choice of Ω (e.g. the solution of MLE in a class of smooth densities) and a threshold ϵ , in-distribution generalisation occurs when the learned policy π_θ returns the unseen demonstrator’s action for a state $\mathbf{x} \notin \mathcal{D}$, but with $\Omega(\mathbf{x}) \geq \epsilon$. We can thus introduce an in-distribution manifold $\hat{\mathcal{X}} = \{\mathbf{x} \in \mathcal{X} \mid \Omega(\mathbf{x}) \geq \epsilon\}$. Similarly, we define

Definition 1 (OOD generalisation, informal). A policy π is capable of OOD generalisation if its error is low for arbitrary states $\mathbf{x} \notin \mathcal{D}$ such that $\Omega(\mathbf{x}) \leq \epsilon$.

Let us consider a desired manifold of states $\mathcal{X}^* \supset \hat{\mathcal{X}}$ including OOD data points. In general, a policy trained through BC on \mathcal{D} will not generalise to \mathcal{X}^* , as supervised learning assumes that the training and test data is iid. Further assumptions on the problem space are thus needed to enable OOD generalisation.

IV. PROBLEM SPACE TRANSFORMATIONS

In order to enable OOD generalisation over \mathcal{X}^* , we propose to apply a transformation $\mathcal{T} : \mathcal{P} \rightarrow \mathcal{Q}$, and thus introduce a transformed problem space \mathcal{Q} over which the policy is learned¹. Let $\hat{\pi}_\theta$ be the minimiser of the empirical BC loss over the transformed dataset $\mathcal{T}(\mathcal{D}) = \{(\mathcal{T}(\mathbf{x}, \mathbf{a}) \mid (\mathbf{x}, \mathbf{a}) \in \mathcal{D})\}$. The goal of this transformation is to maximise data coverage over the desired manifold²: $\min_{\mathcal{T}} |\mathcal{T}(\mathcal{X}^*) \setminus \mathcal{T}(\hat{\mathcal{X}})|$, while ensuring that the BC solution can recover the demonstrator’s actions from the transformed state space: $\pi_d(\mathbf{x}) \approx \mathcal{T}^{-1}(\hat{\pi}_\theta(\mathcal{T}(\mathbf{x}))) \forall \mathbf{x} \in \hat{\mathcal{X}}$. We visualise this operation in Figure 2. Intuitively, while the objective can be optimised by “removing information” (e.g. via a low-rank linear projection), the constraint ensures that any task-relevant information is retained. If

¹To ease notation, we will overload \mathcal{T} to also operate over states and actions separately.

² $|\cdot|$ represents an n -dimensional volume or Lebesgue measure.

the demonstrator π_d fulfils certain assumptions, then the problem space may contain irrelevant information, and the objective can be optimised. It is important to highlight that the just stated objective is introduced as an explanatory device: in this work we don’t propose that the optimisation be solved analytically or numerically. In the following, we discuss practical assumptions which we use to derive transformations which minimise the stated objective, without guarantees that these transformations are strictly optimal.

A. Practical Assumptions for Robotic Manipulation

This work leverages two assumptions. First, a well-known property of many manipulation demonstrations is equivariance to transformations in $\text{SE}(n)$ (where n is equal to 2 or 3, depending on the problem dimension) with respect to (w.r.t.) to a fixed world frame \mathcal{W} . For example, in picking up an object with a parallel gripper, what is relevant is the relative location of the gripper to the object, not the absolute location in \mathcal{W} . The second assumption is that object manipulation often affects objects *locally*. As a consequence, it is often sufficient to have complete information about the surroundings of the EE. For example, the exact position and orientation of an entity are not decisive when the EE is further away from the object than a distance $\lambda \in \mathbb{R}^+$. This distance λ is task specific, and excessively low values might make the demonstrator’s policy irrecoverable in the transformed problem space. Nonetheless, for most tasks, we hypothesise that an appropriate value can easily be determined.

B. Applying Assumptions in Problem Space

a) *Transformation \mathcal{T}_1* : The first transformation we consider encodes $\text{SE}(n)$ equivariance to changes of the entities’ poses w.r.t. to a fixed world frame \mathcal{W} , where \mathcal{W} measures the state values in a Cartesian coordinate system with fixed origin, denoted as \mathcal{W} (e.g., at the base of the robot arm). A state $\mathbf{x} \in \mathcal{X}$ can be expressed as $\mathbf{x} = [\mathcal{W}\mathbf{x}_r, \mathcal{W}\mathbf{x}_{o,1}, \dots, \mathcal{W}\mathbf{x}_{o,N_o}]$, where the prescript denotes the frame in which the state is measured. Actions are expressed analogously $\mathbf{a} = [\mathcal{W}\mathbf{a}_r]$. We propose to transform \mathcal{X} to a frame \mathcal{E} matching the position and the orientation of the end-effector. This induces a transformed state $\mathcal{T}_1(\mathbf{x}) = [\mathcal{E}\mathbf{x}_r, \mathcal{E}\mathbf{x}_{o,1}, \dots, \mathcal{E}\mathbf{x}_{o,N_o}]$. Any action³ $\mathbf{a} \in \mathcal{A}$ is also transformed accordingly: $\mathcal{T}_1(\mathbf{a}) = [\mathcal{E}\mathbf{a}_r]$. This ensures that interactions between end-effector and entities may have the same representation, regardless of poses in the fixed coordinate frame \mathcal{W} . In turn, this can increase the density of the occupancy over the transformed state space, effectively enlarging the in-distribution manifold. An important aside to \mathcal{T}_1 : For some MDP modelling choices, an additional entity corresponding to a fixed point (usually the target position) in \mathcal{W} needs to be added to \mathcal{X} when transforming the problem space to frame \mathcal{E} such that the demonstrator’s policy remains recoverable.

³This transformation can be applied no matter if the action is supplied as a next EE position, an offset to the current position or as a velocity, though the exact transformation varies.

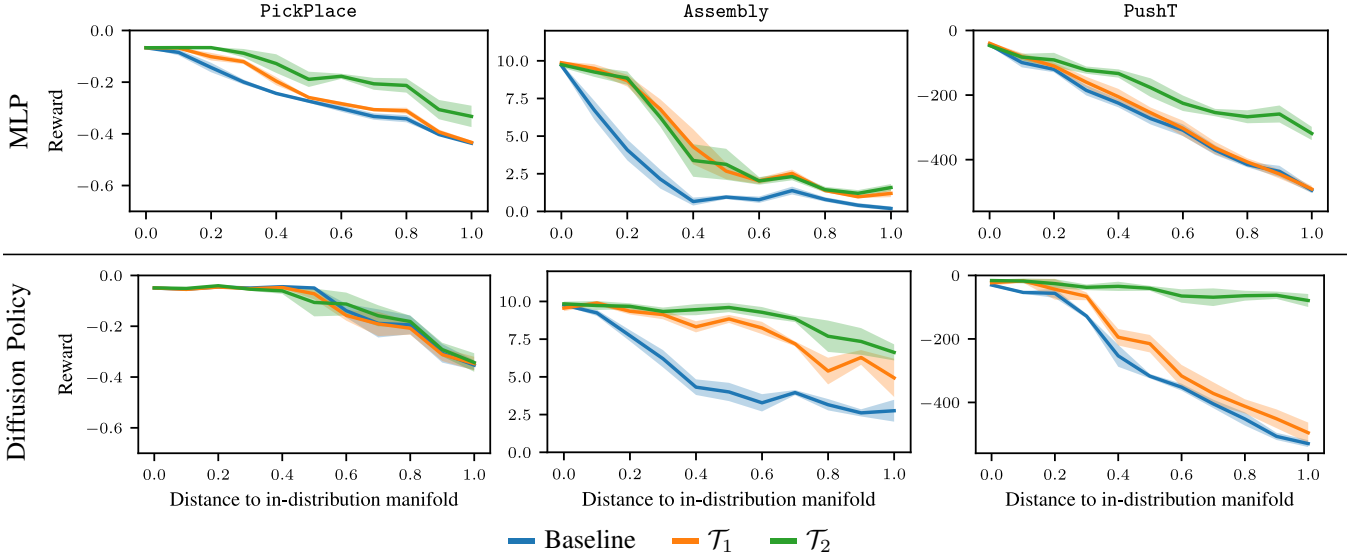


Fig. 3. Comparison of BC policies trained in the original problem space \mathcal{P} , in $\mathcal{T}_1(\mathcal{P})$ and $\mathcal{T}_2(\mathcal{P})$ on in-distribution and OOD initial states. Top row is for policies trained with MLP, bottom row is for policies trained with diffusion policies. The x-axis shows the normalised distance to the in-distribution manifold, where the value at 0 represents the in-distribution performance. The y-axis shows the mean and standard deviation of final rewards across seeds (higher reward is better).

b) *Transformation \mathcal{T}_2* : The second transformation we consider encodes the assumption that manipulation largely occurs locally. Starting from the output of \mathcal{T}_1 , we introduce a parameter $\lambda \in \mathbb{R}^+$ and project the position of each entity $\mathbf{x}_{o,i}$ with $i \in [1, \dots, N_O]$ to the surface of the λ -ball centred in the origin:

$$\text{proj}(\mathbf{x}_{o,i}) = \begin{cases} (\text{pos}(\mathbf{x}_{o,i}), \text{rot}(\mathbf{x}_{o,i})), & \text{if } \|\text{pos}(\mathbf{x}_{o,i})\|_2 < \lambda \\ \left(\frac{\lambda \text{pos}(\mathbf{x}_{o,i})}{\|\text{pos}(\mathbf{x}_{o,i})\|_2}, \text{rot}(\mathbf{x}_{o,i}) \right), & \text{otherwise} \end{cases} \quad (1)$$

where $\text{pos}(\cdot)$ and $\text{rot}(\cdot)$ denote the positional and orientational parts of the object pose vectors, respectively. For $(\mathbf{x}, \mathbf{a}) \in \mathcal{X} \times \mathcal{A}$, the transformation \mathcal{T}_2 can thus be written as

$$\begin{aligned} \mathcal{T}_2(\mathbf{x}) &= [\text{proj}(\mathcal{E}\mathbf{x}_r), \text{proj}(\mathcal{E}\mathbf{x}_{o,1}), \dots, \text{proj}(\mathcal{E}\mathbf{x}_{o,N_O})], \\ \mathcal{T}_2(\mathbf{a}) &= [\mathcal{E}\mathbf{a}_r]. \end{aligned} \quad (2)$$

Small values of λ can greatly reduce the size of the transformed desired manifold $\mathcal{T}_2(\mathcal{X}^*)$ (i.e., by “clipping” it), and thus maximise data coverage over it. As long as the demonstrator is concerned with local information (i.e., it is invariant to the distance of entities that are further away than λ), its policy can be recovered after the transformation. On the other hand, if λ is too small, an arbitrary policy might be irrecoverable as \mathcal{T}_2 effectively loses information (i.e., on the exact position of distant entities).

c) *Notes on Practical Implementation*: When predicting a single action from a single observation, i.e. when $T_X = T_A = 1$, in both \mathcal{T}_1 and \mathcal{T}_2 the pose of the end-effector in frame \mathcal{E} , $\mathcal{E}\mathbf{x}_r$, can be dropped, as it is a zero vector and identity orientation. When using a method to predict an action trajectory from a trajectory of states, the pose of the end-effector is retained, as not all steps will contain trivial information. Slight care needs to be taken for selecting which end-effector pose is used to determine frame \mathcal{E} . We propose that the pose of the most current time step is used. While we propose that the end-effector pose $\mathcal{E}\mathbf{x}_r$ is projected in

eq. (2), as in principle this follows from the assumption, just like the projection of the other state entries, in practice the state horizons T_X are short, and thus the projection would not have an effect. In the experiments (see section V) this is the case as well, thus we cannot provide any experimental data on the effect of the projection on $\mathcal{E}\mathbf{x}_r$.

V. EXPERIMENTAL RESULTS

In this section we want to understand how BC policies perform in-distribution and OOD, in the baseline problem space \mathcal{P} , and in those defined by the proposed transformations. We first consider three simulated tasks which fulfil our assumptions on the problem-type to evaluate the effect of the transformations on OOD generalisation. While we focus on simulated experiments as they allow better control over experimental conditions, we complete our empirical evaluation on a real-world task in Section V-E, which confirms simulated results on hardware.

A. Evaluation Tasks

a) *Meta-World Tasks*: In `PickPlace` and `Assembly`, the demonstrator controls the position of the end-effector of a 7-DOF robot arm in a 3D environment. Both tasks are adapted from the Meta-World benchmark [36].

In `PickPlace`, the task is to move a block from an arbitrary initial position to a goal position fixed above the table. We modify the task by replacing the object from the original cylinder to a cube. The policy only controls the end-effector position for this task, the commanded end-effector orientation is fixed (this is as is given in the benchmark). The demonstration data is collected using the scripted policy provided by the benchmark.

In `Assembly`, the task is to pick up a tool with a handle and a loop and then to place the tool with the loop around the peg. We modify the environment compared to benchmark to make the task more realistic. The position and orientation of the tool are randomised at initialisation.

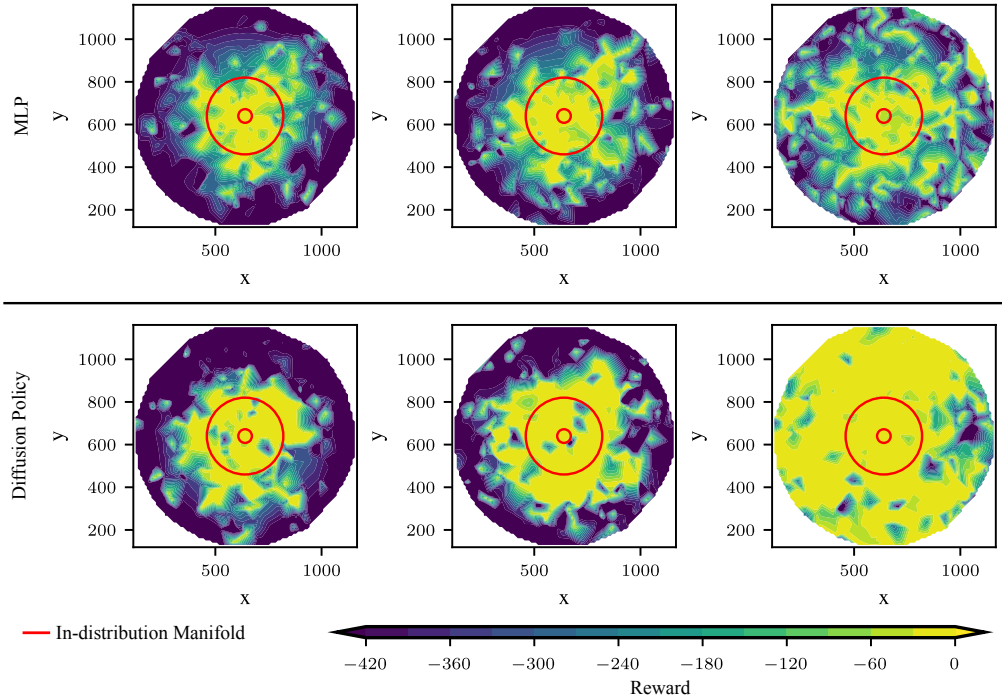


Fig. 4. Comparison of Baseline \mathcal{P} (left), $\mathcal{T}_1(\mathcal{P})$ (middle) and $\mathcal{T}_2(\mathcal{P})$ (right) for `PushT`. Plot colour indicates (interpolated) reward per initial object position averaged over seeds. The top row shows the results for an MLP, the bottom row for diffusion policies. The in-distribution manifold lies within the red torus (between the inner and outer circle), the OOD manifold outside of the outer red circle. The plot in all cases visualises the baseline problem space \mathcal{P} .

The policy controls the 3D position of the end-effector and a subspace of the orientation. While the end-effector orientation command given to the environment is fixed such that it stays parallel to the table, the policy commands the rotation angle α in that plane. The demonstration data is provided by a scripted policy, which was modified based on the one provided by the benchmark.

b) PushT Environment: `PushT` is a simulated 2D environment, where the demonstrator controls a 2D point mass end-effector, adapted from [3]. We have modified the environment compared to the version presented in [3]. The task is to move the T from its initial pose to the goal position at the centre of the environment. A constant point on the T needs to reach the target - unlike the goal in [3], the final pose can be arbitrary. The demonstration data is collected by a human demonstrator. A visualisation of all three task environments is shown in Figure 5.

B. Evaluation Methodology

We test the effectiveness of our proposed problem space transformations when learning a BC policy with two different BC methods. The first method is the naive approach to train a policy which maps a single state to a single action by minimising the mean-squared error of the policy predictions

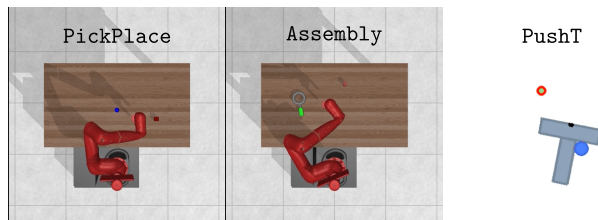


Fig. 5. A rendering of the three simulation environments considered in our evaluation.

using MLPs. The second method is to predict a trajectory of actions from a trajectory of states using a transformer-based diffusion policy approach, as proposed in [3]. The basic experimental setup is the same for all environments. A manifold of the state space is defined and used to sample initial states. Demonstrations are collected starting from these sampled initial distributions. At test time the learned policies are tested by initialising the environments at a fixed set of initial states. To measure in-distribution performance these initial states are sampled in the same region as that used in data collection. OOD performance is measured by sampling initial states which lie in a region which doesn't intersect with the data collection manifold. We train policies with both policy classes on the baseline problem space \mathcal{P} , on the problem space transformed into the end-effector space $\mathcal{T}_1(\mathcal{P})$ and on the problem space additionally transformed using the projection $\mathcal{T}_2(\mathcal{P})$. The same model hyperparameters per task and policy representation are used per task to ensure correct comparison. Implementation details for the learning algorithms and hyperparameters can be found in Section VI-A. Details on the datasets and the in-distribution and OOD manifold specifications are in Section VI-B.

C. Main Results

Figure 3 reports the final rewards for all tasks and problem spaces, as a function of the distance of the initial configuration with respect to those for which data was collected. From left to right, the initial position of entities (e.g. T, cube or ring with handle) is sorted into bins (for evaluation purposes only), which expand concentrically from the in-distribution manifold. From left to right per plot we report the mean reward per initial state bin with the normalised distance from the in-distribution manifold reported on the x-axis. The value at distance zero represents the in-distribution

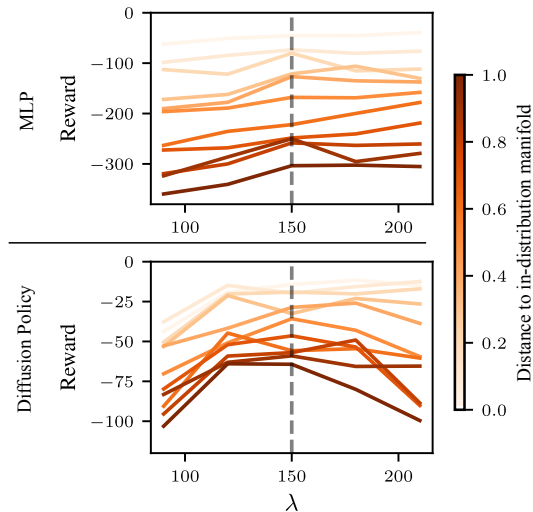


Fig. 6. Ablation of λ (in pixels) for `PushT` on in-distribution and OOD performance. BC with MLP above and Diffusion Policy below. The dotted line represents the value selected for the experiments.

performance while the others represent OOD bins with increasing distance. The distances are reported on a normalised axis, though they are not equal for all tasks. We report the results both for an MLP policy and Diffusion Policy. For both policy types, the in-distribution validation performance is similar in all three problem spaces. For both policy types all problem spaces display some performance degradation moving from in-distribution to the maximum OOD bin. In certain cases \mathcal{T}_1 is able to aid OOD generalisation. At the same time, \mathcal{T}_2 performs at least equally as well as either other problem space and in some cases significantly better, which highlights the relative importance of locality to $SE(n)$ equivariance.

In Figure 4, the heat map of final rewards per initial object (T) position in `PushT` is shown, providing a detailed comparison between the three problem spaces for both policy classes. The plots always visualise the baseline problem space \mathcal{P} . In general it can be seen that Diffusion Policy is better able to learn the task than the naive MLP policy representation, already for the in-distribution region. While the policy is able to successfully complete the task for initial states of the object which lie on the fringes of the in-distribution manifold in \mathcal{P} , it generally fails not far beyond. The performance improves for \mathcal{T}_1 , while \mathcal{T}_2 is able to successfully execute tasks far outside the in-distribution manifold. This is especially visible for BC trained with Diffusion Policy, where in the transformed problem space $\mathcal{T}_2(\mathcal{P})$ high reward is achieved for most initial states - in-distribution as well as OOD. Heat maps for `PickPlace` and `Assembly` can be found in Section VI-C.

D. Ablations

The main hyperparameter introduced by the proposed method is the projection range λ . It must be large enough to retain enough information about the local manipulation task, while keeping it as small as possible to boost OOD performance. Of course, a λ value tending towards infinity means that \mathcal{T}_2 loses its effect, and the performance will

match \mathcal{T}_1 . In our experiments, λ had to generally be just large enough such that the geometry of the object and its interaction with target position doesn't produce values greater than the projection radius. At the same time the radius should be kept small enough that it ideally causes in-distribution states to be projected to the λ -ball, and thus cover it. For both policy classes, we run an ablation over a range of λ values with three random seeds per value. For diffusion policies it can clearly be seen that small λ values hurt in-distribution performance (and hence also OOD performance), while large λ values reduce OOD performance while the in-distribution performance remains constant. For the MLP policy representation, the conclusion from the ablation is not as clear, due to the general decrease in performance of the policy. Nevertheless, we can observe that an excessively small λ remains detrimental.

E. Real-World Evaluation

We finally evaluate our approach on a real-world robotic hardware setup to validate the results obtained in simulation. Experiments are conducted on a real-world variant of the `PushT` task, which differs from the simulated environment and poses additional challenges due to sensing noise and actuation errors.

The task is executed on a single-arm ALOHA robot platform [6]. Training data is collected via teleoperation by a single expert demonstrator. Consistent with the simulation experiments, the policy receives state-based observations as input. The pose of the T-shaped object is estimated using an Apriltag-based tracking system with two calibrated RGB webcams. An overview of the hardware setup is shown in Figure 7.

For the real-world evaluation, we exclusively consider behaviour cloning (BC) with a diffusion policy, due to higher reported performance on hardware [3]. OOD performance results on the physical robot are summarized in Table I. For each policy, we execute 15 rollouts from uniformly sampled initial states, drawn from both an in-distribution (ID) set and an out-of-distribution (OOD) set. The object is initialised in as similar a location as possible across all compared transformation to ensure fair comparison. The first metric we show is the distance from the target the T object should be pushed towards for all three transformations, a lower number is better. The second metric shows how much closer to the goal the object is at termination compared to its initial position, as despite best efforts the exact initial state locations varies between rollouts. The third metric represents the same number as the second metric, though it shows the relative distance moved towards the goal.

Consistent with the simulation results, we observe a clear performance improvement when using \mathcal{T}_2 compared to the baseline problem space, demonstrating that the benefits of the problem space transformation apply to real-world robotic execution too. Though, in contrast with simulation results, we see that the performance of \mathcal{T}_1 is reduced compared to the baseline, which in turn means that the increase in



Fig. 7. The real-world one-arm setup (using ALOHA [6]) used to collect teleoperation data and to rollout trained policy (wrist camera is unused).

performance of \mathcal{T}_2 can be traced back to the assumption of locality.

TABLE I
REAL-WORLD EVALUATION

Policy	Baseline	\mathcal{T}_1	\mathcal{T}_2
Mean dist. at termination [m]	0.1977	0.2075	0.1853
Mean dist. moved towards goal [m]	0.0387	0.0292	0.0501
Mean rel. dist. moved towards goal [-]	16.38%	12.32%	21.29%

VI. LIMITATIONS AND CONCLUSION

This work validates the hypothesis that the problem space in which a BC policy is trained has an effect on OOD performance. Moreover, it demonstrates that, by choosing appropriate transformations leveraging practical assumptions of common manipulation problems, broader OOD generalisation can be enabled. Nevertheless, our experimental validation is restricted to tasks with rigid bodies and low-dimensional state information. For instance, the proposed transformations wouldn't be able to directly handle visual input, nor OOD scenarios that would arise in visual data. While this domain lies beyond the scope of this work, we still expect that domain-specific properties might be leveraged to design different problem space transformations. Finally, the reliance on the fact that the data covers the transformed problem space well remains. For these reasons, we suggest that future directions of work could focus on determining transformations which are applicable more generally, or data-driven methods which aid in the discovery of transformations.

APPENDIX

A. Implementation Details

a) BC with MLPs: We train the MLP models using PyTorch. The policy is implemented as a deterministic MLP with ReLU activation functions. We use dropout and L_2 regularisation. The models are trained using mini random batches and all data is standardised to zero mean and one standard deviation before being passed to the neural network.

The loss function is the 2-norm between policy prediction and dataset sample. The Adam optimizer is used to update the weights. Training time for all tasks is in the order of minutes, while evaluation in simulation is on the order of 10 minutes. The hyperparameters used in training the models is shown in Table II.

TABLE II
TRAINING HYPERPARAMETERS USED WHEN TRAINING MLP BC POLICY FOR THE DIFFERENT TASKS.

Task	PickPlace	Assembly	PushT
Hidden Layers	5	5	5
Hidden Dimen.	512	512	512
Dropout prob.	0.05	0.05	0.05
Regularisation weight	1e-5	1e-5	1e-5
Learning Rate	1e-3	1e-3	1e-3
Batch Size	512	512	1024
Epochs	600	600	1200

b) BC with Diffusion Policy: We use a PyTorch implementation of Diffusion Policy based on the openly available implementation provided by the authors. We follow the same approach to training the models as described in [3] using the transformer-based variant. Training time for all tasks with our implementation is on the order of 10 hours, though significant speed up would be possible with a more efficient implementation of the transformations. The hyperparameters used in training are shown in Table III. The table differentiates between the number of predicted action steps T_{A_p} and the number of action steps which are then executed before policy inference is performed again T_{A_e} . To deploy the diffusion policy on a real system we follow [3] by using DDIM noise scheduling and reducing the number of diffusion steps at inference to 16 (100 steps in training) compared with using DDPM noise scheduling in training and testing at 100 diffusion steps for the simulation tasks.

TABLE III
TRAINING HYPERPARAMETERS USED WHEN TRAINING DIFFUSION POLICY FOR THE DIFFERENT TASKS.

Task	PickPlace	Assembly	PushT	PushT Real
T_X	2	2	2	2
T_{A_p}	10	10	16	16
T_{A_e}	8	8	8	6
Layers	8	8	8	8
Learning Rate	1e-4	1e-4	1e-4	1e-4
Batch Size	256	256	256	256
Epochs	5010	1800	5010	1750
Attn. Dropout	0.3	0.3	0.01	0.1

B. Task and Experiment Details

The main task and experiment specific parameters are summarised in Table IV. The specified in-distribution and OOD manifolds relate to the position of the relevant object of the task. For `PickPlace`, `Assembly` and `PushT Real` the in-distribution manifold is a rectangle and the OOD manifold is a larger rectangle excluding the in-distribution

TABLE IV
SUMMARY OF TASK AND EXPERIMENT RELEVANT PARAMETERS.

Task	PickPlace	Assembly	PushT	PushT Real
# Demonstrations	100	200	200	200
Collected by	Scripted Policy	Scripted Policy	Human Demonstrator	Human Demonstrator
# In-dist. evaluation episodes	100	100	100	15
# OOD evaluation episodes	450	450	400	15
In-dist. manifold obj. pos.	$x_1 \in [-0.15, 0.15]\text{m}$, $x_2 \in [0.48, 0.62]\text{m}$	$x_1 \in [-0.15, 0.15]\text{m}$, $x_2 \in [0.43, 0.67]\text{m}$	$r \in [32, 180]\text{px}$, $\theta \in [0, 2\pi]\text{rad}$	$x_1 \in [0.31, 0.61]\text{m}$, $x_2 \in [-0.15, 0.15]\text{m}$
OOD manifold obj. pos.	$x_1 \in [-0.465, 0.465]\text{m}$, $x_2 \in [0.4, 0.7]\text{m}$	$x_1 \in [-0.465, 0.465]\text{m}$, $x_2 \in [0.38, 0.72]\text{m}$	$r \in [180, 534]\text{px}$, $\theta \in [0, 2\pi]\text{rad}$	$x_1 \in [0.2, 0.71]\text{m}$, $x_2 \in [-0.225, 0.225]\text{m}$
λ (for \mathcal{T}_2)	0.1m	0.2m	150px	0.225m
# Experiment Seeds MLP	8	8	8	-
# Experiment Seeds DP	5	5	5	1
Reward	Distance to target	See implementation [36]	Distance to target	Distance to target
Action Space	[EE Pos., Gripper Force]	[EE Pos., 1D EE Orientation, Gripper Force]	[EE Pos. (2D)]	[EE Pos., EE Orient. (quaternion), Norm. Gripper Pos.]

manifold. The parameters of these rectangles are provided in Cartesian coordinates in the table. For `PushT`, they are sampled from a torus with inner and outer radius in both cases, the parameters in the table are provided in cylindrical coordinates. In all cases the end-effector is initialised at the same pose. For `Assembly`, `PushT` and `PushT Real` the orientation of the relevant object is randomised in $[0, 2\pi]$ in training and evaluation, but for `PickPlace` the initial orientation of the object is constant.

C. Additional Results

Section VI-C shows the heat map results for `PickPlace` and `Assembly`.

ACKNOWLEDGMENT

K.D. extends his gratitude to Núria Armengol, Yijiang Huang and Miguel Zamora for valuable and insightful discussions. M.B. is supported by the Max Planck ETH Center for Learning Systems.

REFERENCES

- [1] M. Bain and C. Sammut, "A framework for behavioural cloning," in *Machine Intelligence*, vol. 15, 1995.
- [2] S. Ross and D. Bagnell, "Efficient reductions for imitation learning," in *AISTATS*, 2010.
- [3] C. Chi, S. Feng, Y. Du, Z. Xu, E. Cousineau, B. Burchfiel, and S. Song, "Diffusion policy: Visuomotor policy learning via action diffusion," in *Proceedings of Robotics: Science and Systems (RSS)*, 2023.
- [4] T. Z. Zhao, J. Tompson, D. Driess, P. Florence, S. K. S. Ghasemipour, C. Finn, and A. Wahid, "ALOHA unleashed: A simple recipe for robot dexterity," in *8th Annual Conference on Robot Learning*, 2024. [Online]. Available: <https://openreview.net/forum?id=gvdXE7ikHI>
- [5] A. O'Neill, A. Rehman, A. Maddukuri, A. Gupta, A. Padalkar, A. Lee, A. Pooley, A. Gupta, A. Mandlkar, A. Jain *et al.*, "Open x-embodiment: Robotic learning datasets and rt-x models: Open x-embodiment collaboration 0," in *2024 IEEE International Conference on Robotics and Automation (ICRA)*. IEEE, 2024, pp. 6892–6903.
- [6] T. Z. Zhao, V. Kumar, S. Levine, and C. Finn, "Learning fine-grained bimanual manipulation with low-cost hardware," *arXiv preprint arXiv:2304.13705*, 2023.
- [7] S. Ross, G. Gordon, and D. Bagnell, "A reduction of imitation learning and structured prediction to no-regret online learning," in *Proceedings of the Fourteenth International Conference on Artificial Intelligence and Statistics*, ser. Proceedings of Machine Learning Research, G. Gordon, D. Dunson, and M. Dudík, Eds., vol. 15. Fort Lauderdale, FL, USA: PMLR, 11–13 Apr 2011, pp. 627–635. [Online]. Available: <https://proceedings.mlr.press/v15/ross11a.html>
- [8] M. Laskey, J. Lee, R. Fox, A. Dragan, and K. Goldberg, "Dart: Noise injection for robust imitation learning," in *Conference on robot learning*. PMLR, 2017, pp. 143–156.
- [9] S. Belkhal, Y. Cui, and D. Sadigh, "Data quality in imitation learning," *Advances in Neural Information Processing Systems*, vol. 36, 2024.
- [10] C. Zhang, S. Bengio, M. Hardt, B. Recht, and O. Vinyals, "Understanding deep learning (still) requires rethinking generalization," *Communications of the ACM*, vol. 64, no. 3, pp. 107–115, 2021.
- [11] J. Liu, Z. Shen, Y. He, X. Zhang, R. Xu, H. Yu, and P. Cui, "Towards out-of-distribution generalization: A survey," *arXiv preprint arXiv:2108.13624*, 2021.
- [12] S. Schaal, "Is imitation learning the route to humanoid robots?" *Trends in cognitive sciences*, vol. 3, no. 6, pp. 233–242, 1999.
- [13] T. Osa, J. Pajarinen, G. Neumann, J. A. Bagnell, P. Abbeel, J. Peters *et al.*, "An algorithmic perspective on imitation learning," *Foundations and Trends® in Robotics*, vol. 7, no. 1-2, pp. 1–179, 2018.
- [14] G.-H. Kim, S. Seo, J. Lee, W. Jeon, H. Hwang, H. Yang, and K.-E. Kim, "Demodice: Offline imitation learning with supplementary imperfect demonstrations," in *International Conference on Learning Representations*, 2022.
- [15] J. Ho and S. Ermon, "Generative adversarial imitation learning," *Advances in neural information processing systems*, vol. 29, 2016.
- [16] D. Garg, S. Chakraborty, C. Cundy, J. Song, and S. Ermon, "Iq-learn: Inverse soft-q learning for imitation," *Advances in Neural Information Processing Systems*, vol. 34, pp. 4028–4039, 2021.
- [17] A. Kumar, J. Hong, A. Singh, and S. Levine, "When should we prefer offline reinforcement learning over behavioral cloning?" *arXiv preprint arXiv:2204.05618*, 2022.
- [18] A. Block, D. J. Foster, A. Krishnamurthy, M. Simchowitz, and C. Zhang, "Butterfly effects of sgd noise: Error amplification in behavior cloning and autoregression," in *ICLR*, 2024.
- [19] D. J. Foster, A. Block, and D. Misra, "Is behavior cloning all you need? understanding horizon in imitation learning," *arXiv preprint arXiv:2407.15007*, 2024.
- [20] T. Xu, Z. Li, and Y. Yu, "Error bounds of imitating policies and environments," in *NeurIPS*, vol. 33, 2020.
- [21] A. Block, A. Jadbabaie, D. Pfrommer, M. Simchowitz, and R. Tedrake, "Provable guarantees for generative behavior cloning: Bridging low-level stability and high-level behavior," in *NeurIPS*, vol. 36, 2024.
- [22] A. Simeonov, Y. Du, A. Tagliasacchi, J. B. Tenenbaum, A. Rodriguez, P. Agrawal, and V. Sitzmann, "Neural descriptor fields: Se (3)-equivariant object representations for manipulation," in *2022 International Conference on Robotics and Automation (ICRA)*. IEEE, 2022, pp. 6394–6400.
- [23] J. Yang, C. Deng, J. Wu, R. Antonova, L. Guibas, and J. Bohg, "Equivalent: Sim(3)-equivariant visuomotor policies beyond rigid object manipulation," in *2024 IEEE International Conference on Robotics and Automation (ICRA)*, 2024, pp. 9249–9255.
- [24] J. Yang, Z.-a. Cao, C. Deng, R. Antonova, S. Song, and J. Bohg, "Equibot: Sim (3)-equivariant diffusion policy for generalizable and data efficient learning," *arXiv preprint arXiv:2407.01479*, 2024.
- [25] T. Zhang, Y. Hu, J. You, and Y. Gao, "Leveraging locality to

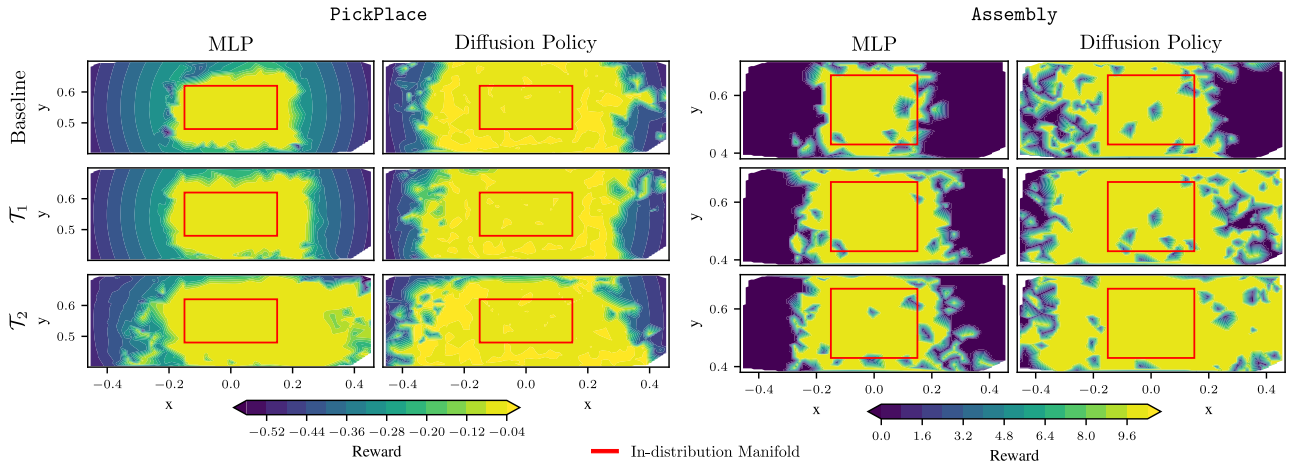


Fig. 8. Heat map of results for `PickPlace` on the left and `Assembly` on the right for all three problem spaces. Plot colour indicates (interpolated) reward per initial object position. The in-distribution manifold lies within the red rectangle, the OOD manifold outside of it for both tasks. The plots in all cases visualise the baseline problem space \mathcal{P} .

- boost sample efficiency in robotic manipulation,” *arXiv preprint arXiv:2406.10615*, 2024.
- [26] R. Takizawa, I. Karino, K. Nakagawa, Y. Ohmura, and Y. Kuniyoshi, “Enhancing reusability of learned skills for robot manipulation via gaze and bottleneck,” *arXiv preprint arXiv:2502.18121*, 2025.
- [27] D. Wang, R. Walters, and R. Platt, “SO(2)-equivariant reinforcement learning,” 2022. [Online]. Available: <https://arxiv.org/abs/2203.04439>
- [28] A. Tangri, O. Biza, D. Wang, D. Klee, O. Howell, and R. Platt, “Equivariant offline reinforcement learning,” *arXiv preprint arXiv:2406.13961*, 2024.
- [29] S. Beery, G. Van Horn, and P. Perona, “Recognition in terra incognita,” in *Proceedings of the European conference on computer vision (ECCV)*, 2018, pp. 456–473.
- [30] M. Arjovsky, L. Bottou, I. Gulrajani, and D. Lopez-Paz, “Invariant risk minimization,” *arXiv preprint arXiv:1907.02893*, 2019.
- [31] D. Krueger, J. Caballero, J.-H. Jacobsen, A. Zhang, J. Binas, D. Zhang, R. Le Priol, and A. Courville, “Out-of-distribution generalization via risk extrapolation (rex),” *arXiv preprint arXiv:2003.00688*, 2021.
- [32] K. Ahuja, T. Lemke, W. Fedus, A. Courville, I. Mitliagkas, and I. Rish, “Invariant risk minimization games,” in *International Conference on Machine Learning*, 2021.
- [33] I. Ahmed, Y. Bengio, M. van der Wilk, and S. Lacoste-Julien, “Systematic generalisation with group invariant predictions,” *arXiv preprint arXiv:2010.06680*, 2021.
- [34] X. Fu, G. Yang, P. Agrawal, and T. Jaakkola, “Learning task informed abstractions,” in *International Conference on Machine Learning*, 2021.
- [35] O. Kroemer, S. Niekum, and G. Konidaris, “A review of robot learning for manipulation: Challenges, representations, and algorithms,” *Journal of Machine Learning Research*, vol. 22, no. 30, pp. 1–82, 2021. [Online]. Available: <http://jmlr.org/papers/v22/19-804.html>
- [36] T. Yu, D. Quillen, Z. He, R. Julian, K. Hausman, C. Finn, and S. Levine, “Meta-world: A benchmark and evaluation for multi-task and meta reinforcement learning,” in *Conference on Robot Learning (CoRL)*, 2019. [Online]. Available: <https://arxiv.org/abs/1910.10897>